A nanoporous graphene analog for superfast heavy metal removal and continuous-flow visible-light photoredox catalysis

Journal Name

COMMUNICATION

A nanoporous graphene analog for superfast heavy metal removal and continuous-flow visible-light photoredox catalysis

Ran Xiao,[a,†] John M. Tobin,[b,†] Meiqin Zha,[a] Yunlong Hou,[a] Jun He,[c] Filipe Vilela,[b,*] Zhengtao Xu[a,*]

Received 00th January 20xx,
Accepted 00th January 20xx

DOI: 10.1039/x0xx00000x

www.rsc.org/

We report a highly recyclable, 2D aromatic framework that offers a unique and versatile combination of photocatalytic activity and heavy metal uptake capability, as well as other attributes crucial for green and sustainable development technologies. The graphene-like open structure consists of fused tritopic aromatic building blocks (i.e., hexaoxotriphenylene and hexaazatrinaphthylene) that can be assembled from readily available industrial materials without the need for transition metal catalysts. Besides fast and strong binding for Pb(II) ions (e.g., removing aqueous Pb ions below the drinkable limit within minutes), the alkaline N-heterocycle units of the robust and porous host is able to catalyse quantitatively Knoevenagel reactions in water. Furthermore, the fused donor-acceptor aromatic π-systems enable environmentally friendly photoredox catalyses (PRC) utilizing the safe and abundant visible light in a commercial flow reactor. Also discussed is a new metric for benchmarking kinetic performance of sorbents in the context of heavy metal removal from drinking water.

Due to their large surface areas, functional diversity and robust reusability, porous polymer frameworks (PPFs) are poised to address critical topics concerning clean environment, renewable energy and sustainable chemical processes.[1] Compared with coordination networks (aka MOFs),[2] the covalent PPFs offer better stability, and can be conveniently assembled without the need of crystallization. Besides the common uses of PPFs in gas sorption/storage and as catalysis supports,[3] conjugated PPFs,[1d, 4] with their extended π-systems, offer distinct advantages for energy storage/delivery,[5] photocatalytic H_2 production,[6] heterogeneous photocatalysis,[7] and other light harvesting applications.[7a, 8]

In spite of the rich functionality, most PPFs were designed to target a single, specific type of application, and a clear gap exists in the research of versatile PPFs that offer multiple capabilities for applications.[9] For example, even though heavy metal removal[10] and photocatalysis[7c, 7d] have been separately accomplished in some PPF systems, none has been reported to simultaneously address these two key sustainability topics on water purification and light harvesting. To promote the development of versatile PPFs for green applications, we here present an easy-to-make system (HOTT-HATN, Fig. 1) that features a broad array of green credentials, making for a notable example in integrating multiple sustainability criteria into the development of porous materials.

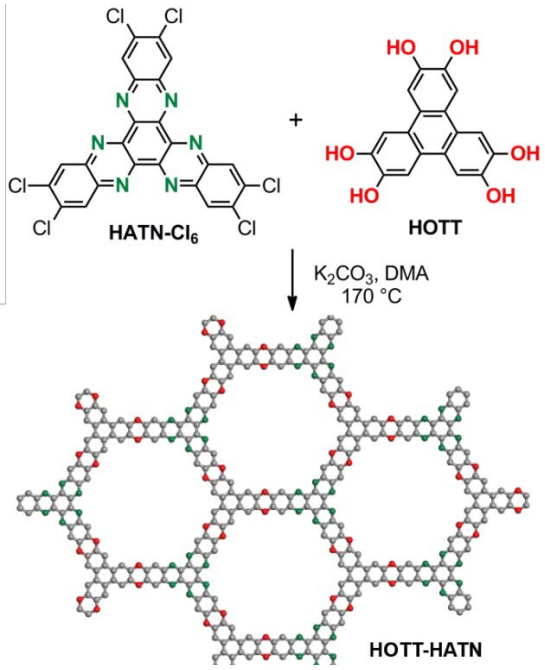

Fig. 1. Synthetic scheme of the honeycomb net of HOTT-HATN (shown in a ball-stick model; red sphere, O; green, N; grey, C).

[a] Department of Biology and Chemistry, City University of Hong Kong, 83 Tat Chee Avenue, Kowloon, Hong Kong. E-Mail: zhengtao@cityu.edu.hk
[b] School of Engineering and Physical Sciences, Heriot-Watt University, Edinburgh, EH14 4AS, United Kingdom. E-Mail: F.Vilela@hw.ac.uk
[c] School of Chemical Engineering and Light Industry, Guangdong University of Technology, Guangzhou 510006, Guangdong, China
† These authors contributed equally to this work.
Electronic Supplementary Information (ESI) available: Synthetic procedures, general experimental method, elemental study, NMR and solid state NMR spectra, IR spectra, TGA curve, PXRD patterns, SEM and TEM images, UV-vis absorption spectrum, Pb absorption kinetic study curve and data tables. See DOI: 10.1039/x0xx00000x

Please do not adjust margins

Besides cleaning up lead ions from water and capturing the safe and abundant visible light for the topical photoredox catalysis (PRC), the HOTT-HATN framework is simply assembled from low-cost building blocks without using toxic or expensive metal catalysts. In addition, the alkaline N donors of the polymer backbone also enables acid-base catalysis using water as a green reaction medium. Moreover, this robust framework can also be deployed as a highly efficient heterogeneous photocatalyst in a commercial flow reactor for optimal separation and recycling advantages. To our knowledge, such a wide-ranging green-chemistry profile remains unprecedented among PPF materials.

On the fundamental level, the fused, fully conjugated aromatic π-system of HOTT-HATN promotes electronic communication throughout the net, providing a versatile 2D electronic platform reminiscent of graphene. Unlike the all-carbon graphene system, the O and N heteroatoms here constitute distinct electron donor-acceptor units. Such D-A units generally exhibit intense photoactivities (e.g., for light harvesting), and were utilized herein to drive photoredox reactions in quantitative yields. Moreover, the chelating pyridinyl N donors on the backbone π-system stand to anchor various metal species, so as to enrich the optical and electronic properties for wider applications.

Results and Discussions

Preparation and analysis of HOTT-HATN

HOTT-HATN was assembled using a high-yield, metal-free aromatic nucleophilic substitution,[9-10, 11] and simply involves heating the two monomers 2,3,6,7,10,11-hexahydroxytriphenylene (HOTT) and 2,3,8,9,14,15-hexachloro-5,6,11,12,17,18-hexaazatrinaphthylene (HATN-Cl_6, Fig. 1) under N_2 at 170°C for five days using K_2CO_3 as the base and DMA as the solvent. After purification *via* Soxhlet extraction, a dark red brown solid was recovered in a high yield (89%).

Results of CHN elemental analysis fits the composition $(C_{42}H_{12}O_6N_6)\cdot(H_2O)_{10}$, with $C_{42}H_{12}O_6N_6$ being that of the 2D net of Fig. 1 (see ESI for details). Energy dispersive X-ray spectra (EDX) reveals only a trace amount of Cl (< 0.2 atom %, Fig. S3), indicating the efficient displacement of the chloro groups.[10a] Thermogravimetric analysis (TGA, Fig. S4) reveals a stable mass up to 250°C, indicating a good thermal stability comparable to other PPFs.[12] The FT-IR peaks (Fig. S5) at 1600 cm^{-1} and at 1200 and 1250 cm^{-1} correspond to the C=N and C-O stretches, respectively. Solid state ^{13}C NMR CP-MAS analysis (Fig. S6) confirmed the fully aromatic system with four dominant peaks at 110.68, 126.27 142.45 and 147.07 ppm, indicating some of the 7 different carbon atoms of HOTT-HATN were not resolved in this measurement. Solid state UV-Vis analysis of the polymer features broad absorbance in the visible spectrum with a λ_{max} at 460 nm (Fig. S7).

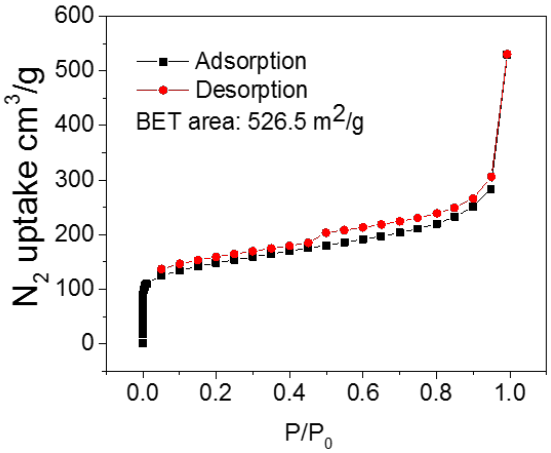

Fig. 2. N_2 isotherm at 77 K of an activated sample of HOTT-HATN.

PXRD established HOTT-HATN as an amorphous solid (Fig. S8), while SEM and TEM images (Fig. S9, S10) revealed highly textured, layer-like morphology. N_2 sorption (at 77 K) experiments confirm the porous character of HOTT-HATN, with a typical type-II N_2 gas adsorption isotherm (Fig. 2) revealing a BET surface area of 526.5 $m^2\cdot g^{-1}$. QSDFT analysis on pore size distribution and pore volume showed an average pore width of 0.52 nm and a micropore volume of 0.579 $cm^3\cdot g^{-1}$ (Fig. S11).

Removal of lead from water

Lead is a cumulative poisonous pollutant that can affect nearly every system in the body. Children under 6 and pregnant women are most susceptible to the negative health effects of lead exposure. The removal of lead and other toxic heavy metals from water sources therefore remains a high priority in the public health sector.[13] In this regard, HOTT-HATN, with its dense array of bipyridine donors (e.g., these are commonly used for metal chelation and catalysis in solution chemistry[14]) offers clear potential. Moreover, the HOTT-HATN powder is freely dispersible in water, which further facilitates green chemistry applications. Such hydrophilicity can be attributed to the polar aza and oxo groups built into the polymer grid. Incidentally, hydrophilicity is rare among PPFs and often has to be achieved through special synthetic design or modification.[15]

The metal uptake studies here follow our long-standing interest in developing metal-binding frameworks for environmental and catalytic applications.[3g, 11a] To probe lead sorption kinetics, a powder sample of HOTT-HATN (20 mg) was added to an aqueous solution of $Pb(NO_3)_2$ (10 ppm; 50 ml) and stirred at room temperature (rt). The Pb remaining in the solution was quantified at specific time intervals *via* ICP-AES. Within 100 seconds the Pb content already dropped below 0.60 ppm, with over 94% of the total Pb removed by the polymer sorbent; within 5 minutes, the Pb content was already reduced beyond the detection limit (15-20 ppb) of the instrument (Table S2, Fig. S12). Such superfast kinetics is on par with a thiol-equipped PPF system for Hg removal (e.g., removing over 99.8% of heavy metal within 5 min, in similar conditions regarding the solvent/sorbate/sorbent ratio),[10b] and can be attributed to the large porosity as well as the distinct hydrophilicity of the O and N components that help the water phase better permeate the polymer matrix. Compared with the thiol-laced PPF systems,[10b, 10c] HOTT-HATN is easier to prepare, and offers better stability, being less prone to oxidation.

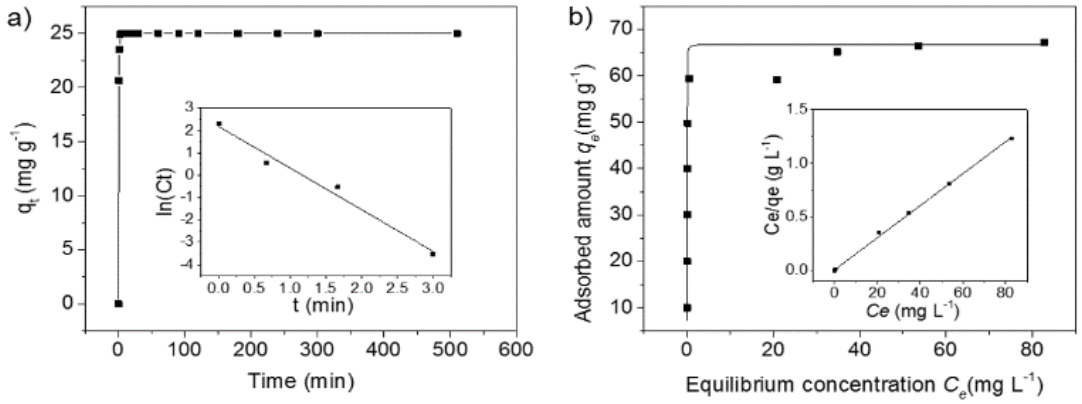

Fig. 3. a) Adsorption curve of Pb(II) versus contact time with HOTT-HATN in aqueous solution. Inset: linear first-order kinetics plot for the initial four points (the Pb levels are below detection limit starting from t = 5 min). b) A Pb(II) Langmuir sorption isotherm for HOTT-HATN. Inset: linear expression fitted with the Langmuir model.

Correct interpretation of kinetics data in adsorption studies is of topical interests (e.g., see Chao's recent review).[16] The present PPF system, with its large porosity and well-defined binding sites, appears fitting for the Langmuir model. The kinetic data indeed fit the first order equation $\ln(C_t) = -k_1 t + \ln(C_i)$ (Fig. 3a inset), which can be rationalized using the Langmuir model $dC_t/dt = kq_tC_t$,[17] where C_t (mg·L^{-1}) refers to the remaining Pb in the solution, q_t the number of unoccupied sites of the sorbent at time t (min), and k (g^{-1}min^{-1}) the rate constant—with q_t approximated to be a constant.

Such an approximation is justified in the present condition, in which excess adsorbent was used so that the sorption sites greatly outnumber the Pb ions, e.g., in the above test the sorbent (20 mg) offers sites for 1.34 mg of Pb uptake, over 2.6 times the Pb ions present (0.5 mg). In general, drinking water treatment usually involves heavy metal pollutants at very low concentrations (e.g., sub-ppm), and the adsorbent is deployed in large excess to fully suppress the residual heavy metal content. In other words, only a small fraction of the binding sites of the adsorbent will be occupied, which further justifies the first order assumption. The linear plot based on the first four data points (the Pb became undetectable by the 5th point) yields a k_1 of 1.86 min^{-1} (Fig. 3a inset), with the corresponding half-life being 0.37 min.

The kinetic data also fit the pseudo-second-order kinetic model[10c, 18] $dq_t/dt = k_{p2}(q_e - q_t)^2$ with the following linear fit:

$$\frac{t}{q_t} = \frac{1}{k_2 q_e^2} + \frac{t}{q_e} \qquad (1)$$

where q_t (mg·g^{-1}) is the amount of Pb adsorbed at time t (min), and q_e (mg·g^{-1}) is the Pb adsorbed at equilibrium, and k_2 (g·mg^{-1}min^{-1}) is the adsorption rate constant (Fig. S13).

Such a fit, however, should be taken with caution.[16a, 16c] Theoretically, the pseudo second order model works best when the total number of the metal ions equals that of the adsorption sites, i.e., $C_iV = q_e$, namely $C_tV = C_iV - q_t = q_e - q_t$, so that $(q_e-q_t)^2 = (C_iV-q_t)(q_e-q_t) = (1/V)(C_i-q_t/V)(q_e-q_t) = (1/V)(C_t)(q_e-q_t)$. When excess sorbent was used (as is often the case), we have $C_iV \ll q_e$ instead and the first order description instead becomes more meaningful.

Second, the linearity between t/q_t and t/q_e is often gratuitous, especially in fast kinetics where $1/(k_2q_e^2)$ is of small, negligible values, rendering $t/q_t \approx t/q_e$. At longer time points, t/q_e becomes ever greater than $1/(k_2q_e^2)$, making the linearity a triviality further devoid of physical significance; also at longer times, the adsorption approaches equilibrium, and the reverse process—the desorption—becomes significant, further invalidating the one-way pseudo second order assumption.[16a] Indeed, with excess adsorbent (i.e., $C_iV \ll q_e$), the q_e value derived from the superficially linear plot between t/q_t and t/q_e is simply the total meal ions present, having nothing to do with the number of available adsorption sites physically present.

To properly assess the sorbent kinetics in connection with the removal of trace heavy metal contaminants, we suggest that excess adsorbent be used in order to mimic the actual deployment of the adsorbent, and to simplify the kinetics to the first order regime. Also, data points should be collected at the early stage so as to avoid the complication from desorption. For example, with the distribution quotient $Q_d = (C_i-C_t)V/C_tm < K_d/100$, the desorption rate is no greater than 1% that of adsorption, and can thus be omitted. As adsorption isotherm is routinely measured, the adsorption capacity q_e and K_d derived thereby provide valuable guidance and cross-check for the kinetic studies. For benchmarking the kinetic performance, the first order rate constant k_1 can be divided by the amount of sorbent m (g). In the above case, k_1/m=1.86/0.020=93 min^{-1}·g^{-1}.

In the isotherm study, a series of 5.0 mL aqueous $Pb(NO_3)_2$ solutions were loaded into glass vials (each containing 5.0 mg HOTT-HATN). The mixtures were shaken at 200 rpm for 4.5 h at rt, then filtered by PTFE membrane. The filtrates were tested *via* ICP-AES. The adsorbed amount of Pb at equilibrium (q_e, mg·g^{-1}) was calculated with the data in Table S3:

$$q_e = \frac{(C_i - C_e) \times V}{m} \qquad (2)$$

where C_i and C_e correspond to initial and equilibrium concentration of Pb in water (mg·L^{-1}), V stands for the solution volume (mL) and m the sorbent mass (g). The adsorption

isotherm plots fit the Langmuir isotherm model (with a correlation coefficient above 0.998; see also Fig. 3b):

$$\frac{C_e}{q_e} = C_e \times \frac{1}{q_{max}} + \frac{1}{K_L q_{max}} \qquad (3)$$

where a plot of C_e/q_e to C_e (see Fig. 3b inset) yields the sorption capacity q_{max} (mg·g^{-1}) as the reciprocal of the slope. The q_{max} value thus obtained (66.8 mg·g^{-1}) is equivalent to 0.28 Pb(II) ion per HATN core, suggesting that a large fraction of bipy donors remain unbonded under these conditions.

The strong affinity for Pb(II) ions is demonstrated by the distribution coefficient (K_d), which is defined as:

$$K_d = \frac{C_i - C_f}{C_f} \times \frac{V}{m} \qquad (4)$$

with C_i and C_f being the initial and final Pb concentrations, V the volume of the solution (mL) and m the amount of sorbent (g). From the isotherm data (e.g., Table S3, Entry 4), K_d was estimated to be greater than 2×10^6 mL·g^{-1}. The effective Pb removal capability is consistent with the strong donor character of the chelating pyridinyl groups. Specifically, such chelating ability is greatly enhanced by the strongly electron-releasing dioxin-like oxo groups built into the conjugated backbone. To better demonstrate the essential role of the nitrogen donors in Pb uptake, a sample of HOTT-HATN polymer was treated with acetic acid to help mask the alkaline pyridinyl sites; consequently, the Pb uptake capacity was found to drop down to about 30 mg·g^{-1} (see Fig. S14), being less than half that of the pristine sample. Such sensitivity of the Pb uptake property to acid treatment indicates that the Pb uptake is effected mostly through the alkaline N donor functions.

Compared with other sorbent systems for Pb removal,[19] the fast kinetics and high K_d value of HOTT-HATN clearly rank among the best, even though the uptake capacity is modest. The extraordinary K_d value, however, is especially useful for removing Pb from drinking water (e.g., down to 15 ppb as is set by the US Environmental Protection Agency).[20] Specifically, with K_d = 2×10^6, for one liter of water with Pb at 150 ppb (i.e., 10 times the legal limit), only 4.5 mg of the HOTT-HATN polymer is needed to reduce the Pb content to 15 ppb. Further to the advantage of product economics, the HOTT-HATN sorbent can be reactivated after stripping off the trapped Pb by sequential washing with the household items of HCl (e.g., 10%), ammonia (5%) and water (see SI for details, e.g., Fig. S15).

The selectivity of heavy metal uptake was examined using a solution containing Hg^{2+}, Pb^{2+}, Cu^{2+}, Cd^{2+} and Zn^{2+} at 4.8-6.4 ppm (see Tables S4, S5), together with Ca^{2+} and Na^{+} at 20 and 53 ppm (to mimic the higher natural occurrence of these two metals), respectively. As shown in Fig. S16, strongest preferences were observed for Hg^{2+}, Cu^{2+}, with over 95% removal achieved within one hour, while the adsorption for Pb^{2+} continues to be effective, with about 90% removal achieved in spite of the various competing ions present at higher concentrations. Notably, the large majority of the low-toxicity ions of Zn^{2+}, Ca^{2+} and Na^{+} were not adsorbed, pointing to further relevance for drinking water treatment. The uptake of the toxic Cd^{2+} ions, however, was only modest, with 65% of the Cd^{2+} ions found to persist in the solution in these experimental conditions.

Knoevenagel condensation reactions

We now explore HOTT-HATN for green and sustainable uses in chemical syntheses. Besides convenient product separation (generally associated with heterogeneous catalysts), its metal-free nature resolves the metal leaching and contamination issue that besets especially electronic and pharmaceutical industries.[6b] The hydrophilicity of HOTT-HATN (e.g., dispersible in water), together with its oxo-strengthened pyridinyl donors, also makes for efficient water-based heterogeneous organocatalysis. The well-known Knoevenagel condensation offers a useful test reaction, because it is amenable to base catalysis, and it is an important C-C bond formation method for fine chemicals and pharmaceuticals.[21]

Table 1. Knoevenagel condensation of aldehydes with malononitrile catalyzed by HOTT-HATN[a]

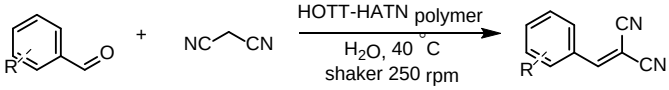

Entry	Aldehyde	Reaction time (h)	Conversion (%)[b]
1	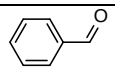	2.5	>99
2[c]	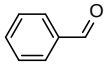	12	67
3[d]	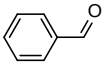	12	80
4[e]	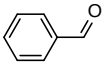	2.5	62
5[f]	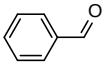	2.5	>99
6	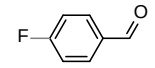	2.5	>99
7	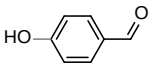	3	>99
8	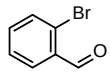	3	>99
9	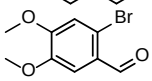	3	>99
10	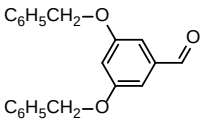	15	82

[a]Reaction conditions: aldehyde (0.25 mmol), malononitrile (0.375 mmol), H_2O (1.0 mL), $CHCl_3$ (0-0.2 mL), HOTT-HATN (5 mg), mechanical shaker (250 rpm), 40 °C. [b]Conversion calculated *via* ^{1}H NMR analysis. [c]$CDCl_3$ (no water added), 50 °C by heating block, stirring. [d]Acetonitrile (no water added), 50 °C by heating block, stirring. [e]In water without HOTT-HATN. [f]HOTT-HATN polymer re-used in the 5th cycle.

The Knoevenagel condensations involved adding an aryl aldehyde (0.25 mmol), malononitrile (0.375 mmol) and HOTT-

HATN (5.0 mg) to 1.0 mL of deionized water (with 0.2 mL of $CHCl_3$ added for substrates with poor water solubility). The reaction vessel was then heated to 40 °C and shaken at 250 rpm for 2.5-3 hours, and the conversion rate determined *via* ^{1}H NMR (see ESI). A benchmark reaction was first performed with benzaldehyde, resulting in 100% conversion after 2.5 hours. Also examined are controls for solvents (chloroform and acetonitrile) in the absence of water as well as a reaction in the absence of HOTT-HATN (Table 1). Interestingly, replacing water with pure $CDCl_3$ dramatically slows down the reaction, e.g., even after 12 hours, only 67% conversion was observed, while straight acetonitrile resulted in (slightly higher) 80% conversion in similar conditions. Also, the absence of HOTT-HATN resulted in a much lower yield (i.e., cf entries 1 and 4), verifying HOTT-HATN as a useful organocatalyst.

Substituted benzaldehydes (4-fluoro, 2-bromo, 4-hydroxy and 2-bromo-4,5-dimethoxy) were also tested to open the scope of application. Each of these showed full conversion within 3 hours. The bulkier substrate (3,5-bis(benzyloxy)-benzaldehyde, entry 10), however, showed a lower conversion of 82% even after 15 hours, presumably due to its difficulty in penetrating the HOTT-HATN matrix. Finally, HOTT-HATN was recovered, washed and reused throughout five catalytic cycles of the model reaction. No significant decrease in catalytic activity was observed therein, further establishing HOTT-HATN as a green and reusable heterogeneous catalyst with efficiency comparing favorably with various other systems.[22]

Aerobic photooxidation of benzylamines

Provided with appropriate photocatalysts, light—especially abundant sunlight—offers an attractive alternative energy input (*vis-à-vis* heat) for driving chemical transformations. In spite of various CMP solids studied as photocatalyts for organic reactions, the field remains wide open.[23] For example, rigorously metal-free CMP photocatalysts are rare, and the continuous flow reactors, well-suited to enable scale-up and to overcome other operational challenges of photochemistry, are curiously often left out in CMP photocatalysis studies.

The oxo and aza functions built into the fully conjugated backbone of HOTT-HATN constitute distinct donor-acceptor units that give rise to broad intense absorption in the visible region (Fig. S7), indicating potential photocatalytic activities. The following continuous-flow synthesis using HOTT-HATN as a photocatalyst aims to combine a unique set of green-chemistry merits. The efficient production of imines thus achieved is also of practical interest in the synthesis of nitrogen-rich biologically molecules.[23-24]

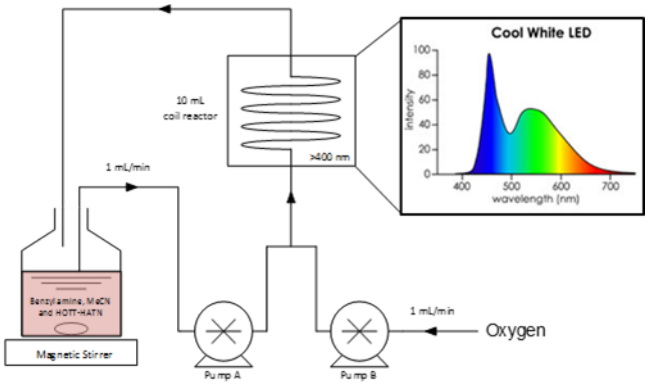

Fig. 4. Schematic representation of the experimental set-up using the easy-Photochem flow reactor from Vapourtec Ltd. with the spectrum for the Cool White LED module (>400 nm).

For the photooxidation, a benzyl amine (0.5 mmol) and HOTT-HATN (5.0 mg, ca 6.5 µmol of the HATT unit) were added to 10 mL of acetonitrile. The suspension was then cycled through a commercial photochemical flow reactor at rt (Vapourtec Ltd., Fig. S17) in the presence of oxygen and visible light (>400 nm, Cool White LED module, Fig. 4) until the amine was consumed. The conversion rate was measured by ^{1}H NMR (see ESI).

Table 2. Aerobic oxidative coupling of benzyl amines photocatalyzed by HOTT-HATN[a]

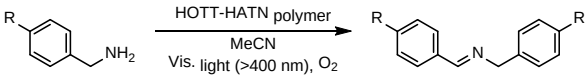

Entry	Amine	Reaction time (h)	Conversion (%)[b]
1	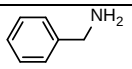	6	>99
2[c]	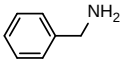	6	2
3[d]	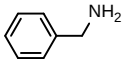	6	14
4[e]	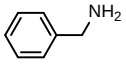	6	-
5[f]	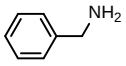	4	>99
6[g]	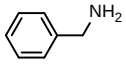	6	92
7	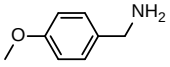	5	>99
8	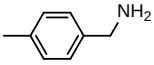	5	>99
9	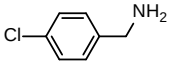	6	>99
10	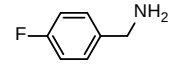	6	>99
11	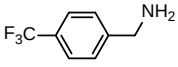	7	>99

[a]Reaction conditions: benzyl amine (0.5 mmol), HOTT-HATN (5.0 mg), acetonitrile (10 mL), 30 °C, visible cool white led module (>400 nm), in flow (1 mL·min^{-1}), O_2 (1 mL·min^{-1}). [b]Conversion calculated *via* ^{1}H NMR spectroscopy. [c]Reaction performed in the absence of light. [d]Reaction performed in the absence of HOTT-HATN. [e]Reaction performed in the absence of O_2, under N_2 atmosphere. [f]Reaction performed using a 420 nm LED module. [g]HOTT-HATN in acetonitrile irradiated for 30 h open to air prior to addition of benzylamine.

As seen in Table 2, a series of benzylic amines were examined. A screening was first performed with benzylamine, resulting in full conversion to the imine product within 6 hours. Control experiments, removing light, photocatalyst or oxygen, were also performed to verify the role of each of these components. Furthermore, heating (at 60°C) under the initial reaction conditions did not significantly change the final conversion of the reactions. The use of a narrow wavelength light source (420 ± 2 nm) reduced the reaction time to 4 h. However, due to the abundance of white light sources (as in household lighting), we opted to continue with the Cool White LED module.

Substituted benzyl amines (4-methoxy, 4-methyl, 4-fluoro, 4-chloro, and 4-trifluoromethyl) were also tested to probe scope of substrates. While we note some variation in the time required for full conversion, the differences in these times were not greatly significant. Specifically, benzyl amines with electron-donating groups took slightly less time to reach full conversion (5 hours), while those with strong electron-withdrawing groups took longer (7 h). Recently, the photooxidation of benzylamine has been described as proceeding through either a photoredox or singlet oxygen ($^1O_2$) mechanism.[25] Through a photoredox mechanism, the amine substrate transfers an electron to the triplet excited state of HOTT-HATN. The photoreduced HOTT-HATN subsequently interacts with O_2 to form a superoxide radical anion ($O_2^{\cdot-}$), and thus returning to the ground state. The amine radical is then oxidized *via* $O_2^{\cdot-}$, where the intermediate amine is able to react with the initial amine substrate to form the desired product. Conversely, the production of $^1O_2$ proceeds *via* an energy transfer between O_2 and the triplet excited state of HOTT-HATN. The amine substrate is then oxidized by $^1O_2$ and proceeds to the product in a similar manner as described for the photoredox mechanism.

To better understand how the reaction proceeds, the ability for HOTT-HATN to be used for the production of $^1O_2$ was investigated through the conversion of α-terpinene to ascaridole, as described in our previous work.[26] After 2 h irradiation with a Cool While LED Module (>400 nm), the reaction showed a 62 % conversion to the ascaridole product *via* ^{1}H NMR spectroscopy, indicating $^1O_2$ production under experimental conditions similar to those presented for the photooxidation experiments. Therefore, we can reasonably conclude that the photooxidation of benzylamines is most likely proceeding through a $^1O_2$ mechanism.

Lastly, we investigated both the photostability and productivity of HOTT-HATN. To test the material for photostability, HOTT-HATN was added to acetonitrile and irradiated for 30 hours in the presence of oxygen. The irradiated suspension was then used for the model reaction where 92% conversion was achieved within 6 h, establishing that HOTT-HATN maintains high catalytic activity, and therefore photostability, even after prolonged exposure to high intensity light. FTIR analysis of the polymer before and after 36 h of intense irradiation (Fig. S37) presented with virtually no change, further indicating the stability of HOTT-HATN. We also note that $^1O_2$ is generated throughout the entirety of the irradiation period, cementing HOTT-HATN as not only photostable, but also inert under highly oxidative conditions. Furthermore, with the same amounts of HOTT-HATN (5.0 mg) and solvent, the benzylamine can be raised in concentration (from 0.05) up to 0.08 mmol·mL^{-1} and still demonstrate full conversion within 6 hours (higher concentrations require longer reaction time), equivalent to a TON above 120. Overall, the photocatalytic activity of HOTT-HATN compares well with other photocatalysts (both metal-rich and metal-free) for oxidative coupling of benzyl amines.[23]

Conclusions

In conclusion, an impressive array of green credentials has been achieved from a highly reusable, fused-aromatic framework efficiently assembled via a transition-metal-free substitution reaction between the building blocks of HOTT and HATN-Cl_6. In particular, the oxo and the aza sites built into the conjugated polymer backbone provide a powerful electron donor-acceptor couple that effects the photocatalysis of aerobic amine oxidation using visible light when applied in a commercial flow reactor. Moreover, the oxo units also enhance the basicity of the pyridinyl aza units, so as to effectively catalyze the Knoevenagel reaction in water, and aid in the speedy removal of Pb from water to acceptable drinking levels set by worldwide environmental organizations. This latter capability is especially of note not only because of the convenient recyclability of the polymer matrix (e.g., by washing with HCl), but also because of the widespread presence of lead as a pollutant in the environment.

Acknowledgements

This work is supported by a GRF grant of Research Grants Council of Hong Kong SAR (Project 11303414), the National Natural Science Foundation of China (21471037) and Guangdong Natural Science Funds for Distinguished Young Scholars (15ZK0307). We acknowledge Vapourtec Ltd for their technical support.

References

1. a) S. Das, P. Heasman, T. Ben and S. Qiu, *Chem. Rev.*, 2017, **117**, 1515-1563; b) D. Wu, F. Xu, B. Sun, R. Fu, H. He and K. Matyjaszewski, *Chem. Rev.*, 2012, **112**, 3959-4015; c) P. Kaur, J. T. Hupp and S. T. Nguyen, *ACS Catal.*, 2011, **1**, 819-835; d) Y. Xu, S. Jin, H. Xu, A. Nagai and D. Jiang, *Chem. Soc. Rev.*, 2013, **42**, 8012-8031; e) N. Chaoui, M. Trunk, R. Dawson, J. Schmidt and A. Thomas, *Chem. Soc. Rev.*, 2017, **46**, 3302-3321.
2. a) C. Wang, D. Liu and W. Lin, *J. Am. Chem. Soc.*, 2013, **135**, 13222-13234; b) M. Zhang, Z.-Y. Gu, M. Bosch, Z. Perry and H.-C. Zhou, *Coord. Chem. Rev.*, 2015, **293-294**, 327-356; c) V. Guillerm, D. Kim, J. F. Eubank, R. Luebke, X. Liu, K. Adil, M. S. Lah and M. Eddaoudi, *Chem. Soc. Rev.*, 2014, **43**, 6141-6172; d) P. Deria, J. E. Mondloch, O. Karagiaridi, W. Bury, J. T. Hupp and O. K. Farha, *Chem. Soc. Rev.*, 2014, **43**, 5896-5912; e) D. J. Tranchemontagne, Z. Ni, M. O'Keeffe and O. M. Yaghi, *Angew. Chem., Int. Ed.*, 2008, **47**, 5136-5147; f) J. He, M. Zeller, A. D. Hunter and Z. Xu, *CrystEngComm*, 2015, **17**, 9254-9263.

3. a) F. Goettmann, A. Fischer, M. Antonietti and A. Thomas, *Angew. Chem. Int. Ed.*, 2006, **45**, 4467-4471; b) Y. Zhang, Y. Zhang, Y. L. Sun, X. Du, J. Y. Shi, W. D. Wang and W. Wang, *Chem. Eur. J.*, 2012, **18**, 6328-6334; c) C. Lu, T. Ben and S. Qiu, *Macromol. Chem. Phys.*, 2016, **217**, 1995-2003; d) L. Chen, Y. Yang and D. Jiang, *J. Am. Chem. Soc.*, 2010, **132**, 9138-9143; e) L. Chen, Y. Yang, Z. Guo and D. Jiang, *Adv. Mater.*, 2011, **23**, 3149-3154; f) R. Palkovits, M. Antonietti, P. Kuhn, A. Thomas and F. Schüth, *Angew. Chem. Int. Ed.*, 2009, **48**, 6909-6912; g) J. Liu, J. M. Tobin, Z. Xu and F. Vilela, *Polym. Chem.*, 2015, **6**, 7251-7255; h) P. Zhang, Z. Weng, J. Guo and C. Wang, *Chem. Mater.*, 2011, **23**, 5243-5249.
4. J.-X. Jiang, F. Su, A. Trewin, C. D. Wood, N. L. Campbell, H. Niu, C. Dickinson, A. Y. Ganin, M. J. Rosseinsky, Y. Z. Khimyak and A. I. Cooper, *Angew. Chem. Int. Ed.*, 2007, **46**, 8574-8578.
5. F. Vilela, K. Zhang and M. Antonietti, *Energy Environ. Sci.*, 2012, **5**, 7819-7832.
6. a) G. Zhang, Z.-A. Lan and X. Wang, *Angew. Chem. Int. Ed.*, 2016, **55**, 15712-15727; b) R. S. Sprick, J.-X. Jiang, B. Bonillo, S. Ren, T. Ratvijitvech, P. Guiglion, M. A. Zwijnenburg, D. J. Adams and A. I. Cooper, *J. Am. Chem. Soc.*, 2015, **137**, 3265-3270; c) K. Kailasam, M. B. Mesch, L. Moehlmann, M. Baar, S. Blechert, M. Schwarze, M. Schroeder, R. Schomaecker, J. Senker and A. Thomas, *Energy Technol.*, 2016, **4**, 744-750.
7. a) Y.-L. Wong, J. M. Tobin, Z. Xu and F. Vilela, *J. Mater. Chem. A*, 2016, **4**, 18677-18686; b) Z. Xie, C. Wang, K. E. de Krafft and W. Lin, *J. Am. Chem. Soc.*, 2011, **133**, 2056-2059; c) J. Luo, X. Zhang and J. Zhang, *ACS Catal.*, 2015, **5**, 2250-2254; d) J.-X. Jiang, Y. Li, X. Wu, J. Xiao, D. J. Adams and A. I. Cooper, *Macromolecules*, 2013, **46**, 8779-8783.
8. C. Gu, N. Huang, Y. Chen, L. Qin, H. Xu, S. Zhang, F. Li, Y. Ma and D. Jiang, *Angew. Chem. Int. Ed.*, 2015, **54**, 13594-13598.
9. J. Liu, K.-K. Yee, K. K.-W. Lo, K. Y. Zhang, W.-P. To, C.-M. Che and Z. Xu, *J. Am. Chem. Soc.*, 2014, **136**, 2818-2824.
10. a) P. M. Budd, B. Ghanem, K. Msayib, N. B. McKeown and C. Tattershall, *J. Mater. Chem.*, 2003, **13**, 2721-2726; b) B. Li, Y. Zhang, D. Ma, Z. Shi and S. Ma, *Nat. Commun.*, 2014, **5**, 5537; c) Q. Sun, B. Aguila, J. Perman, L. D. Earl, C. W. Abney, Y. Cheng, H. Wei, N. Nguyen, L. Wojtas and S. Ma, *J. Am. Chem. Soc.*, 2017, **139**, 2786-2793; d) N. Huang, L. Zhai, H. Xu and D. Jiang, *J. Am. Chem. Soc.*, 2017, **139**, 2428-2434.
11. a) J. Liu, J. Cui, F. Vilela, J. He, M. Zeller, A. D. Hunter and Z. Xu, *Chem. Commun.*, 2015, **51**, 12197-12200; b) N. Du, G. P. Robertson, I. Pinnau and M. D. Guiver, *Macromolecules*, 2009, **42**, 6023-6030; c) A. R. Oveisi, K. Zhang, A. Khorramabadi-zad, O. K. Farha and J. T. Hupp, *Sci. Rep.*, 2015, **5**, 10621.
12. Y. Xu, S. Jin, H. Xu, A. Nagai and D. Jiang, *Chem. Soc. Rev.*, 2013, **42**, 8012-8031.
13. P. B. Tchounwou, C. G. Yedjou, A. K. Patlolla and D. J. Sutton, *EXS*, 2012, **101**, 133-164.
14. C. Kaes, A. Katz and M. W. Hosseini, *Chem. Rev.*, 2000, **100**, 3553-3590.
15. a) H. Urakami, K. Zhang and F. Vilela, *Chem. Commun.*, 2013, **49**, 2353-2355; b) B. C. Ma, S. Ghasimi, K. Landfester, F. Vilela and K. A. I. Zhang, *J. Mater. Chem. A*, 2015, **3**, 16064-16071; c) S. Ghasimi, K. Landfester and K. A. I. Zhang, *ChemCatChem*, 2016, **8**, 694-698.
16. a) H. N. Tran, S.-J. You, A. Hosseini-Bandegharaei and H.-P. Chao, *Water Res.*, 2017, **120**, 88-116; b) W. Plazinski, W. Rudzinski and A. Plazinska, *Adv. Colloid Interface Sci.*, 2009, **152**, 2-13; c) G. Alberti, V. Amendola, M. Pesavento and R. Biesuz, *Coord. Chem. Rev.*, 2012, **256**, 28-45.
17. S. Azizian, *J. Colloid Interface Sci.*, 2004, **276**, 47-52.
18. a) R. Rostamian, M. Najafi and A. A. Rafati, *Chem. Eng. J.*, 2011, **171**, 1004-1011; b) Y.-S. Ho, *J. Hazard. Mater.*, 2006, **136**, 681-689.
19. a) J. Li, X. Liu, Q. Han, X. Yao and X. Wang, *J. Mater. Chem. A*, 2013, **1**, 1246-1253; b) A. Mahapatra, B. Mishra and G. Hota, *J. Hazard. Mater.*, 2013, **258**, 116-123; c) W. Li, D. Chen, F. Xia, J. Z. Tan, J. Song, W.-G. Song and R. A. Caruso, *Chem. Commun.*, 2016, **52**, 4481-4484; d) S. Zhang, H. Yang, H. Huang, H. Gao, X. Wang, R. Cao, J. Li, X. Xu and X. Wang, *J. Mater. Chem. A*, 2017, **5**, 15913-15922; e) H. Saleem, U. Rafique and R. P. Davies, *Microporous Mesoporous Mater.*, 2016, **221**, 238-244; f) Y. Ni, L. Jin, L. Zhang and J. Hong, *J. Mater. Chem.*, 2010, **20**, 6430-6436.
20. Lead Free Water, World Standards for allowable levels of lead in water, http://leadfreewater.com/world-standards/, (accessed March 16, 2017).
21. a) L. R. Madivada, R. R. Anumala, G. Gilla, S. Alla, K. Charagondla, M. Kagga, A. Bhattacharya and R. Bandichhor, *Org. Process Res. Dev.*, 2009, **13**, 1190-1194; b) C. A. Martinez, S. Hu, Y. Dumond, J. Tao, P. Kelleher and L. Tully, *Org. Process Res. Dev.*, 2008, **12**, 392-398; c) S. D. Walker, C. J. Borths, E. DiVirgilio, L. Huang, P. Liu, H. Morrison, K. Sugi, M. Tanaka, J. C. S. Woo and M. M. Faul, *Org. Process Res. Dev.*, 2011, **15**, 570-580.
22. a) B. Li, M. Chrzanowski, Y. Zhang and S. Ma, *Coord. Chem. Rev.*, 2016, **307**, 106-129; b) W. Ge, X. Wang, L. Zhang, L. Du, Y. Zhou and J. Wang, *Catal. Sci. Technol.*, 2016, **6**, 460-467; c) E. M. Schneider, M. Zeltner, N. Kranzlin, R. N. Grass and W. J. Stark, *Chem. Commun.*, 2015, **51**, 10695-10698; d) J. Gascon, U. Aktay, M. D. Hernandez-Alonso, G. P. M. van Klink and F. Kapteijn, *J. Catal.*, 2009, **261**, 75-87; e) T. I. Reddy and R. S. Varma, *Tetrahedron Lett.*, 1997, **38**, 1721-1724.
23. B. Chen, L. Wang and S. Gao, *ACS Catal.*, 2015, **5**, 5851-5876.
24. S.-I. Murahashi, *Angew. Chem. Int. Ed. Engl.*, 1995, **34**, 2443-2465.
25. a) A. Berlicka and B. Konig, *Photochem. Photobiol. Sci.*, 2010, **9**, 1359-1366; b) N. Kang, J. H. Park, K. C. Ko, J. Chun, E. Kim, H.-W. Shin, S. M. Lee, H. J. Kim, T. K. Ahn, J. Y. Lee and S. U. Son, *Angew. Chem. Int. Ed.*, 2013, **52**, 6228-6232.
26. J. M. Tobin, J. Liu, H. Hayes, M. Demleitner, D. Ellis, V. Arrighi, Z. Xu and F. Vilela, *Polym. Chem.*, 2016, **7**, 6662-6670.